Preprints of the 19th World Congress
The International Federation of Automatic Control
Cape Town, South Africa. August 24-29, 2014

Interval Arithmetic based Influence Analysis on Power Flow caused by Integration of Wind Power and Electric Vehicles

Lizi Luo*, Junpeng Zhu*, Shengchun Yang, Ke Wang**, Jianguo Yao**, Wei Gu***

* School of Electrical Engineering, Southeast University, Nanjing 210096, China
(e-mail: luolizi@126.com, zhujp_0705@163.com, wgu@seu.edu.cn).
** China Electric Power Research Institute, Nanjing 210003, China
(e-mail: yangshengchun@epri.sgcc.com.cn, wangke@epri.sgcc.com.cn, yaojianguo@epri.sgcc.com.cn).

Abstract: With the increasing scale of renewable generations and uncertain loads that connected to power systems, the uncertainties of power injections in both source side and load side have become significant, due to their randomness and intermittency. How to model the uncertainties with an appropriate method and analyse the influence of uncertainties on power flow has become the basis of power system planning and operation. This paper proposes interval models for wind power and electric vehicles, and then applies an interval arithmetic-based algorithm to analyse the influence on power flow caused by the uncertainties. IEEE 30-bus test system with integration of wind power and electric vehicles is used as a simulation example to analyse the influence in details.

1. INTRODUCTION

Power flow analysis is one of the most fundamental and most frequently used tools in power system analysis both for planning and operation. It deals with the calculation of voltages and line flows based on the given network parameters and load injections. Traditionally, all of the parameters in power flow equations are certain values which never change over time and many classical algorithms have been proposed to calculate the power flow, such as Newton-Raphson and Fast Decoupled algorithms. However, with the increasing scale of renewable generations and uncertain loads connected to power systems, power injections at some buses have become to be significant uncertainties, which make it difficult for the traditional deterministic method to calculate the power flow. How to model the uncertainties and choose an appropriate algorithm to calculate the uncertain power flow is the key to analyse the uncertainties' influence on power flow.

Three modelling approaches have been reported to analyse the problems of uncertainties, which respectively are probability analysis, fuzzy sets and interval arithmetic (Dimitrovski & Tomsovic, 2004). In probability analysis, uncertainties are represented by probability distribution functions. However, quantitative probability distribution function is not given objectively and mainly depended on the historical data or assumptions. As a result, the inherent error in probability function may bring larger error to the results. In fuzzy sets, uncertainties are represented as fuzzy numbers and calculated according to the fuzzy number algorithm. The membership functions of the uncertain parameters are needed when utilizing fuzzy sets, while the membership function is not given objectively. Compared with probability distribution function, setting membership functions includes more subjective factors. In interval arithmetic, uncertainties are expressed using two boundary values, which are upper bound and lower bound respectively. Interval doesn't contain any extra information, thus avoiding subjective factors in the calculation results. Furthermore, compared with the above modelling approaches, interval arithmetic has a faster speed because of its less information, which is very important in some applications like power flow analysis.

This paper presents interval models of wind power and electric vehicles, which are respectively typical renewable generation and uncertain load. After modelling the uncertainties, interval arithmetic is employed to carry out power flow analysis with the integration of wind power and electric vehicles.

The organization of this paper is as follows. In Section 2, interval models of wind power and electric vehicles are presented. Section 3 applies the interval arithmetic-based algorithm for power flow analysis. Simulation results are analysed in Section 4 to describe the influence on power flow caused by integration of wind power and electric vehicles. Lastly, Section 5 concludes this paper.

2. INTERVAL MODELS OF WIND POWER AND ELECTRIC VEHICLES

As typical renewable generation and uncertain load, wind power and electric vehicles are respectively analysed in this section.

2.1 Interval Models of Wind Power

The output of a wind farm is considered to be related to the third power of the wind speed

$$P_R = N\frac{\rho}{2}C_p\pi R^2 v_R^3$$
$$P_W(v) = \begin{cases} 0 & v \le v_{ci} \text{ or } v \ge v_{co} \\ \frac{P_R}{v_R^3 - v_{ci}^3}v^3 - \frac{v_{ci}^3}{v_R^3 - v_{ci}^3}P_R & v_{ci} \le v \le v_R \\ P_R & v_R \le v \le v_{co} \end{cases} \quad (1)$$

where $P_w(v)$ is the wind power when the wind speed is v and P_R is the rated power. N is the number of wind turbines, ρ is the air density, C_p is the energy conversion efficiency, R is the radius of the wind turbine blade, v_R is the rated wind speed. v_{ci} is the cut-in wind speed and v_{co} is the cut-out wind speed.

The interval model of wind power should be built according to the random characteristic of wind speed. Wind speed follows a Weibull distribution (Hetzer *et al.*, 2008):

$$f(V_w) = \frac{k}{\mu}(\frac{V_w}{\mu})^{k-1}e^{-(\frac{V_w}{\mu})^k} \quad (2)$$

where κ is the shape parameter and μ is the predicted value of the wind speed.

An interval which meets the following two conditions is needed to describe the uncertainty of wind power: (1) there is a high enough possibility that the wind power lies within the interval, (2) the interval length should not be too large (at least it is finite). So the interval $[P_w^{down}, P_w^{up}]$ is created using the following formulation:

$$prob(P_w \in [P_w^{down}, P_w^{up}]) = 1 - 2\varepsilon_w \quad (3)$$

where $prob(A)$ is the probability that event A is true, and ε_w is a coefficient related to probability that the wind power lies out the interval, which is usually set between 0.01 and 0.25. Considering the P_w^{down} and P_w^{up} is hard to be calculated analytically according to the probability distribution of wind power, they could be calculated using Monte-Carlo method. Due to the asymmetry of wind power output, the interval $[P_w^{down}, P_w^{up}]$ is always asymmetrical about the predicted output of wind power so as to make the interval have a smaller range.

Assuming the power factor of a wind farm is a constant, the reactive power of wind farm can be calculated using

$$Q_w = \frac{P_w}{\cos\theta_w}\sin\theta_w \quad (4)$$

where $cos\theta_w$ is the power factor. So the $[Q_{down}, Q_{up}]$ can be calculated using $[P_{down}, P_{up}]$.

2.2 Interval Models of Electric Vehicles

Until recently there are three mainstream interactive modes of EVs: normal interaction (NI) mode, fast charging mode and battery exchange (BE) mode. Since the normal interaction EVs are most widely distributed, only NI mode is considered in this paper.

At any given time, demand of NI EVs is mainly influenced by two major factors: the amount of EVs connected to power facilities, the charging power of EVs.

The amount of EVs connected to the power facilities in a given time convert to Poisson distribution $P(\lambda)$ (Yu *et al.*, 2012):

$$prob(N = k) = \frac{\lambda^k}{k!}e^{-\lambda} \quad (5)$$

where λ is the predicted amount of EVs and N represents the practical value.

In order to estimate the possible power demands of connected EVs, an assumption is required: The charging power of a connected EV is considered to be under uniform distribution between 4 to 5 kW.

So at a given time, the power demand of EVs can be calculated as follows:

$$\begin{cases} P_i \sim U(4, 5) \\ N \sim P(\lambda) \\ P_{ev} = \sum_{i=1}^{N} P_i \end{cases} \quad (6)$$

P_{ev} is a stochastic variable whose probability distribution is hard to be calculated, so the Monte-Carlo method is used to set an interval $[P_{ev}^{down}, P_{ev}^{up}]$, which satisfy the following formulation:

$$prob(P_{ev} \in [P_{ev}^{down}, P_{ev}^{up}]) = 1 - 2\varepsilon_{ev} \quad (7)$$

where ε_{ev} is a probability related coefficient.

To make sure the interval is balanced, the formulation can be rewritten as formulation (8):

$$prob(P_{ev} > P_{ev}^{up}) = prob(P_{ev} < P_{ev}^{down}) = \varepsilon_{ev} \quad (8)$$

3. AN INTERVAL ARITHMETIC-BASED ALGORITHM FOR POWER FLOW ANALYSIS

3.1 Interval Arithmetic

A real interval X is a nonempty set of real numbers

$$X = [\underline{x}, \overline{x}] = \{x \in R : \underline{x} \le x \le \overline{x}\} \quad (9)$$

where $\underline{x}$ and $\overline{x}$ are called lower bound and upper bound respectively. If $\underline{x} = \overline{x}$, the interval is called a point interval or thin interval，which stands for a rational number.

Consider two interval numbers $X = [\underline{x}, \overline{x}]$ and $Y = [\underline{y}, \overline{y}]$, addition, subtraction, multiplication, division, intersection and union of these two interval numbers can be described as below (Moore *et al.*, 2009):

Addition: $X+Y=[\underline{x}+\underline{y},\bar{x}+\bar{y}]$ (10)

Subtraction: $X-Y=[\underline{x}-\bar{y},\bar{x}-\underline{y}]$ (11)

Multiplication:

$$X\times Y=[\min(\underline{x}\cdot\underline{y},\ \bar{x}\cdot\bar{y},\ \underline{x}\cdot\bar{y},\ \bar{x}\cdot\underline{y}),\ \max(\underline{x}\cdot\underline{y},\ \bar{x}\cdot\bar{y},\ \underline{x}\cdot\bar{y},\ \bar{x}\cdot\underline{y})] \quad (12)$$

Division:

$$X/Y=[\min(\underline{x}/\underline{y},\ \bar{x}/\bar{y},\ \underline{x}/\bar{y},\ \bar{x}/\underline{y}),\ \max(\underline{x}/\underline{y},\ \bar{x}/\bar{y},\ \underline{x}/\bar{y},\ \bar{x}/\underline{y})] \quad (13)$$

Intersection: $X\cap Y=[\max(\underline{x},\underline{y}),\ \min(\bar{x},\bar{y})]$ (14)

Union: $X\cup Y=[\min(\underline{x},\underline{y}),\ \max(\bar{x},\bar{y})]$ (15)

If either $\underline{x}>\bar{y}$ or $\bar{x}<\underline{y}$, $X\cap Y$ is empty and denoted by ϕ.

3.2 Krawczyk Method Based on Current Injection (Pereira et al., 2012)

Krawczyk method (Mori & Yuihara, 1999) is one of the most heavily used approaches for solving a set of nonlinear equations. Consider a set of nonlinear interval equations

$$f(X)=0 \quad (16)$$

where variable X is an interval vector. Krawczyk operator can be represented as

$$K(X)=x-Y\cdot f(x)+[I-Y\cdot F'(X)](X-x) \quad (17)$$

and the iteration process is shown as below:

$$\begin{cases} X^{k+1}=X^k\cap K(X^k) \\ K(X^k)=x^k-Y^k\cdot f(x^k)+[I-Y^k\cdot F'(X^k)](X^k-x^k) \\ x^k=mid(X^k),\quad Y^k=[mid(F'(X^k))]^{-1} \end{cases} \quad (18)$$

where I is an unit matrix, function *mid(A)* means the midpoint of the interval variable A and $F'(X^k)$ represents the Jacobian matrix with interval elements in iteration k.

Convergence of krawczyk method is related to the infinite norm of matrix R, which in iteration k is represented as

$$R^k=I-Y^k\cdot F'(X^k). \quad (19)$$

Krawczyk method is easy to converge when the infinite norm of R is less than 1 and always get divergence while the infinite norm of R is large. In order to reduce the infinite norm of R, power flow equations based on current injection instead of traditional power injection is chosen to calculate the power flow with the integration of wind power and electric vehicles, which is represented as below:

PQ buses:

$$\Delta I_{rk}=\sum_{i\in\phi_k}(G_{ki}V_{ri}-B_{ki}V_{mi})-\frac{V_{rk}P_k+V_{mk}Q_k}{V_{rk}^2+V_{mk}^2} \quad (20)$$

$$\Delta I_{mk}=\sum_{i\in\phi_k}(G_{ki}V_{mi}+B_{ki}V_{ri})-\frac{V_{mk}P_k-V_{rk}Q_k}{V_{rk}^2+V_{mk}^2} \quad (21)$$

PV buses:

$$\Delta I_{rk}=\sum_{i\in\phi_k}(G_{ki}V_{ri}-B_{ki}V_{mi})-\frac{V_{rk}P_k+V_{mk}Q_k}{V_k^2} \quad (22)$$

$$\Delta I_{mk}=\sum_{i\in\phi_k}(G_{ki}V_{mi}+B_{ki}V_{ri})-\frac{V_{mk}P_k-V_{rk}Q_k}{V_k^2} \quad (23)$$

$$\Delta V_k^2=V_k^2-(V_{rk}^2+V_{mk}^2) \quad (24)$$

where, I_{rk} : real part of current injection at bus k

I_{mk} : imaginary part of current injection at bus k

ϕ_k : set of buses directly connected to bus k

G_{ki} : conductance of branch between bus k and i

B_{ki} : susceptance of branch between bus k and i

V_{rk} : real part of voltage at bus k

V_{mk} : imaginary part of voltage at bus k

V_k : voltage magnitude at bus k

P_k : active power injection at bus k

Q_k : reactive power injection at bus k

According to the current injection equations, Newton-Raphson algorithm is given in Appendix A.

For each PQ bus, the current injection equations contain two variables, V_r and V_m, while for each PV bus, the amount of unknown variables increases to three, which respectively are V_r, V_m and Q. Consequently, Jacobian matrix based on current injection equations has a larger size, although it contributes to decreasing the infinite norm of matrix R and improving the convergence.

3.3 Steps of Power Flow Analysis based on interval arithmetic

Concrete steps of power flow analysis that based on krawczyk method and current injection equations are as follows.

Step 1: Calculate the midpoints of the given interval power injections at all of the buses with uncertainties.

Step 2: Use the midpoints to calculate the deterministic power flow, which would be the basis of the initial values to the power flow analysis with uncertainties.

Step 3: Initialize the real parts and imaginary parts of voltages at all the buses and reactive power injections at PV buses. Actual formulas are

$$V_{rk}=[V_{rk}^d\cdot(1-\delta),V_{rk}^d\cdot(1+\delta)] \quad (25)$$

$$V_{mk}=[V_{mk}^d-V_k\cdot\delta,V_{mk}^d+V_k\cdot\delta)] \quad (26)$$

$$Q_k=[Q_k^d\cdot(1-\delta),Q_k^d\cdot(1+\delta)] \quad (27)$$

where variables with superscript d represent the solutions of deterministic power flow, δ is a percentage stands for a tolerance which make the initial intervals completely contain the power flow solutions.

Step 4: Use the midpoints of interval variables in step 3 to calculate the mismatches of current injections at all the buses and voltages' square value at PV buses according to (20)-(24), which correspond to the column vector in the left of Appendix A.

Step 5: calculate the krawczyk operator using (17).

Step 6: Update the unknown variables with intersection operation according to (18).

Step 7: check whether the solution reach the specified convergent accuracy. After intersection operation in iteration k, to any unknown variable x_i, calculate the distance between x_i^{k-1} and x_i^k, which is denoted by d_i:

$$d_i = \max[\,|\underline{x}_i^k - \underline{x}_i^{k-1}|, |\overline{x}_i^k - \overline{x}_i^{k-1}|\,]. \qquad (28)$$

Use N_{pq} and N_{pv} to represent the amount of PQ and PV buses respectively. If $\max(d_i), i=1,2,\cdots,2N_{pq}+3N_{pv}$, is less than the specified convergent accuracy, the power flow analysis is converged, otherwise the algorithm goes back to Step 4 to proceed with next iteration.

4. SIMULATION RESULTS

IEEE 30-bus test system is used to analyse the influence on power flow caused by the integration of wind power and electric vehicles. Different scenarios are calculated and analysed as below.

Scenario A: Assume the buses numbered 7, 12 and 21 in IEEE 30-bus test system are connected with different wind generations. At each selected bus, the predicted wind power injection is 6MW and coefficient ε_w is 0.05. Based on the current predication level, wind power injections are calculated to have a tolerance of -50% to +33%, more specific, they vary in the range [3MW, 8MW]. Suppose the power factor $cos\theta_w$ is 0.8, then the reactive power range is [2.25MVar, 6MVar]. The power flow solutions obtained by the interval arithmetic-based algorithm are compared with that of deterministic power flow analysis in Fig. 1-2, with Fig. 1 showing the bus voltage magnitude bounds and Fig. 2 depicting the bus voltage angle bounds.

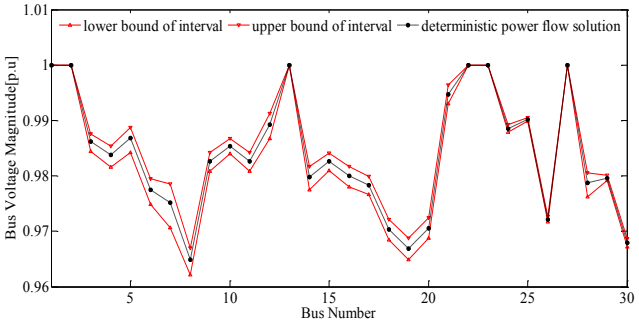

Fig. 1 Bus voltage magnitude bounds of scenario A

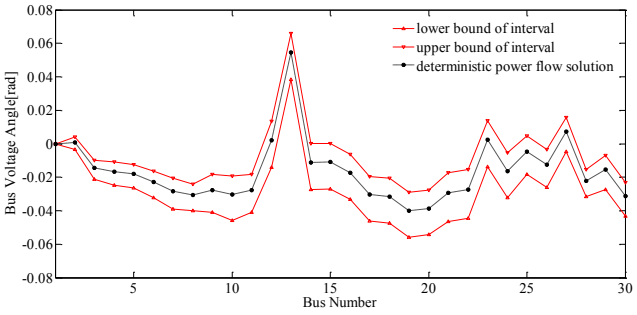

Fig. 2 Bus voltage angle bounds of scenario A

Scenario B: Assume the buses numbered 4, 10, 14, 15, 24 and 30 are connected with EV charging stations. At each selected bus, suppose the predicted EV amount is 1000 and the total load is 4.5MW, which is regarded as a part of the original load in the test system. Set the coefficient ε_{ev} as 0.05 and the tolerance of load can be analysed through the interval models of EVs, which as a result is -5.3% to +5.3%, thus the load of each EV charging station varies in the range [4.26MW, 4.74MW]. The computed interval arithmetic-based solutions are compared with the deterministic power flow solutions in Fig. 3 and Fig. 4, which correspond to the bus voltage magnitude bounds and the bus voltage angle bounds respectively.

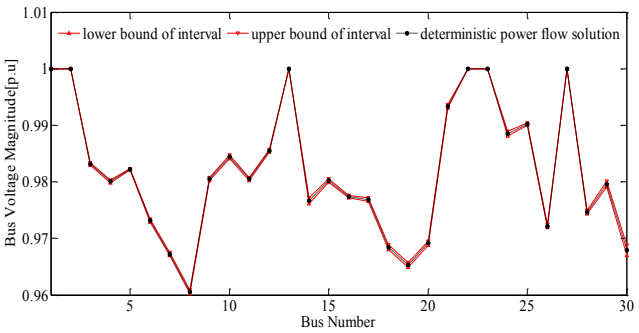

Fig. 3 Bus voltage magnitude bounds of scenario B

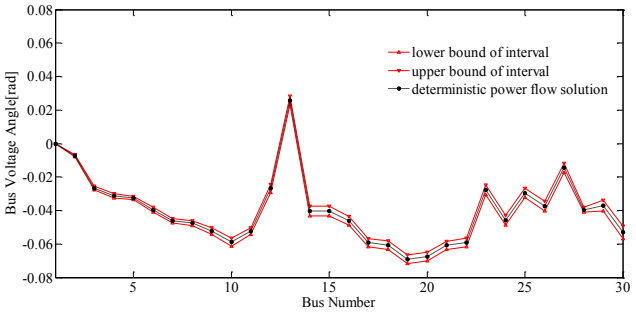

Fig. 4 Bus voltage angle bounds of scenario B

Scenario C: Both of wind power and electric vehicles are considered in this scenario. Based on IEEE 30-bus test system, nine buses are assumed to be connected with uncertainties, which respectively are the three buses with

wind power in scenario A and the six buses with EVs in scenario B. For the models of wind power and electric vehicles, different coefficient ε (ε_w or ε_{ev}) corresponds to different intervals, which would result in different power flow solutions. ε ranged from 0.05 to 0.25 is analysed in this scenario and the solutions are shown in Fig. 5-6.

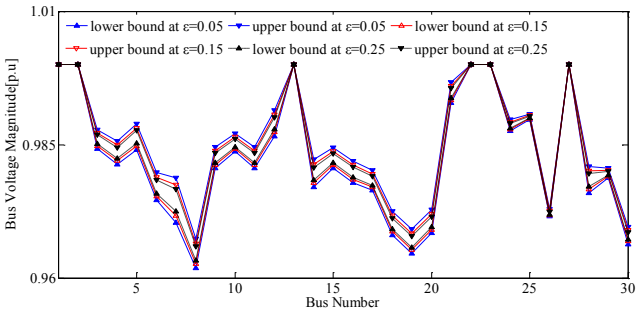

Fig. 5 Bus voltage magnitude bounds at different ε

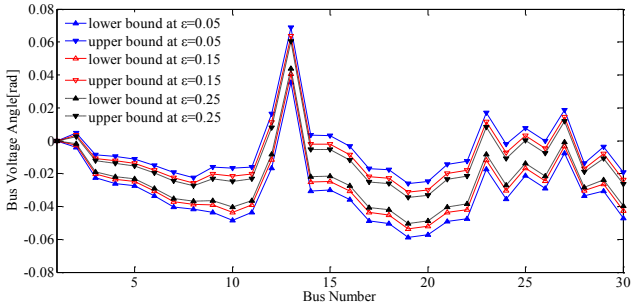

Fig. 6 Bus voltage angle bounds at different ε

Obviously, the power flow solutions have turned into intervals with lower and upper bounds due to the uncertainties at some buses. Ranges of the interval solutions in scenario A is asymmetrical about the deterministic power flow solutions, which result from the asymmetry of interval models of wind power. While in scenario B, both of the EVs' load and solution ranges are almost symmetrical. Notice also that the solution ranges of the system connected with wind power is larger of that connected with EVs when the coefficient ε takes the same value. On one hand, it because that the predicted power injections of wind are larger than EVs', on the other hand, the current predication method of EVs is more accuracy than that of wind power, in other words, wind power has a greater uncertainty than EVs under the current predication level.

With different requirements and applications for uncertain models, different value of coefficient ε should be chosen. ε represents the probability that the given interval model containing the actual power injection and smaller ε corresponds to larger ranges of interval models. For example, ε equals to 0.05 means the interval model have a probability of 90% to contain the actual power injection while 0.25 stands for 50%. In scenario C, ε ranged from 0.05 to 0.25 is analysed. It can be easily observed that the solution bounds increasingly deviate from deterministic power flow solutions as the value of ε decreases, which is same with the variation of the ranges of interval models.

5. CONCLUSIONS

Taking into consideration the uncertainties of renewable generations and uncertain loads, an interval arithmetic-based algorithm is applied to analyse the influence on power flow caused by the uncertainties. As typical renewable generation and uncertain load, interval models of wind power and electric vehicles are presented in this paper. Based on the above-mentioned interval models, power flow solutions of IEEE 30-bus test system are calculated and three different scenarios are analysed. The presented analysis and simulation results demonstrate that the power flow solutions vary in certain ranges and have the same property of symmetry as the power injections. Furthermore, for the same wind farm or EV charging station, different probabilistic requirements can result in interval models with different ranges, which are important for the power flow analysis and directly determine the ranges of power flow solutions. Future work will be focused on the method to select appropriate probabilistic requirements for different uncertainties thus make the interval power flow solutions have more practical significance.

ACKNOWLEDGMENTS

This work was supported by State Grid Corporation of China (dz71-13-036), the National High Technology Research and Development Program of China (863 Program Grant 2012AA050210), the National Science Foundation of China (51277027), the Natural Science Foundation of Jiangsu Province of China (SBK201122387), the Fund Program of Southeast University for Excellent Youth Teachers, the Southeast University Key Science Research Fund.

REFERENCES

Dimitrovski, A., & Tomsovic, K. (2004). Boundary load flow solutions. *Power Systems, IEEE Transactions on*, **19(1)**, 348-355.

Hetzer, J., Yu, D. C., & Bhattarai, K. (2008). An economic dispatch model incorporating wind power. *Energy Conversion, IEEE Transactions on,* **23(2),** 603-611.

Mori, H., & Yuihara, A. (1999). Calculation of multiple power flow solutions with the Krawczyk method. *In Circuits and Systems, 1999. ISCAS'99. Proceedings of the 1999 IEEE International Symposium on* (**Vol. 5**, pp. 94-97). IEEE.

Moore, R. E., Cloud, M. J., & Kearfott, R. B. (2009). *Introduction to interval analysis*, 7-14, Siam.

Pereira, L. E. S., Da Costa, V. M., & Rosa, A. L. S. (2012). Interval arithmetic in current injection power flow analysis. *International Journal of Electrical Power & Energy Systems*, **43(1),** 1106-1113.

Yu, H. J., Gu, W., Zhang, N., et al. (2012). Economic dispatch considering integration of wind power generation and mixed-mode electric vehicles. *In Power*

and Energy Society General Meeting, 2012 IEEE (pp. 1-7). IEEE.

Appendix A.

$$\begin{bmatrix} \Delta I_{m1} \\ \Delta I_{m2} \\ \vdots \\ \Delta I_{mm} \\ \Delta I_{mm+1} \\ \vdots \\ \Delta I_{mn} \\ \Delta I_{r1} \\ \Delta I_{r2} \\ \vdots \\ \Delta I_{rm} \\ \Delta I_{rm+1} \\ \vdots \\ \Delta I_{rn} \\ \Delta V_{m+1}^2 \\ \vdots \\ \Delta V_n^2 \end{bmatrix} = \begin{bmatrix} B_{11}^{'} & B_{12} & \cdots & B_{1m} & B_{1m+1} & \cdots & B_{1n} & G_{11}^{'} & G_{12} & \cdots & G_{1m} & G_{1m+1} & \cdots & G_{1n} & 0 & \cdots & 0 \\ B_{21} & B_{22}^{'} & \cdots & B_{2m} & B_{2m+1} & \cdots & B_{2n} & G_{21} & G_{22}^{'} & \cdots & G_{2m} & G_{2m+1} & \cdots & G_{2n} & 0 & \cdots & 0 \\ \vdots & \vdots & \vdots & \vdots & \vdots & \vdots & \vdots & \vdots & \vdots & \vdots & \vdots & \vdots & \vdots & \vdots & \vdots & \vdots & \vdots \\ B_{m1} & B_{m2} & \cdots & B_{mm}^{'} & B_{mm+1} & \cdots & B_{mn} & G_{m1} & G_{m2} & \cdots & G_{mm}^{'} & G_{mm+1} & \cdots & G_{mn} & 0 & \cdots & 0 \\ B_{m+11} & B_{m+12} & \cdots & B_{m+1m} & B_{m+1m+1}^{'} & \cdots & B_{m+1n} & G_{m+11} & G_{m+12} & \cdots & G_{m+1m} & G_{m+1m+1}^{'} & \cdots & G_{m+1n} & \frac{V_{rm+1}}{V_{m+1}^2} & \cdots & 0 \\ \vdots & \vdots & \vdots & \vdots & \vdots & \vdots & \vdots & \vdots & \vdots & \vdots & \vdots & \vdots & \vdots & \vdots & \vdots & \vdots & \vdots \\ B_{n1} & B_{n2} & \cdots & B_{nm} & B_{nm+1} & \cdots & B_{nn}^{'} & G_{n1} & G_{n2} & \cdots & G_{nm} & G_{nm+1} & \cdots & G_{nn}^{'} & 0 & \cdots & \frac{V_{rn}}{V_n^2} \\ G_{11}^{''} & G_{12} & \cdots & G_{1m} & G_{1m+1} & \cdots & G_{1n} & B_{11}^{''} & -B_{12} & \cdots & -B_{1m} & -B_{1m+1} & \cdots & -B_{1n} & 0 & \cdots & 0 \\ G_{21} & G_{22}^{''} & \cdots & G_{2m} & G_{2m+1} & \cdots & G_{2n} & -B_{21} & B_{22}^{''} & \cdots & -B_{2m} & -B_{2m+1} & \cdots & -B_{2n} & 0 & \cdots & 0 \\ \vdots & \vdots & \vdots & \vdots & \vdots & \vdots & \vdots & \vdots & \vdots & \vdots & \vdots & \vdots & \vdots & \vdots & \vdots & \vdots & \vdots \\ G_{m1} & G_{m2} & \cdots & G_{mm}^{''} & G_{mm+1} & \cdots & G_{mn} & -B_{m1} & -B_{m2} & \cdots & B_{mm}^{''} & -B_{mm+1} & \cdots & -B_{mn} & 0 & \cdots & 0 \\ G_{m+11} & G_{m+12} & \cdots & G_{m+1m} & G_{m+1m+1}^{''} & \cdots & G_{m+1n} & -B_{m+11} & -B_{m+12} & \cdots & -B_{m+1m} & B_{m+1m+1}^{''} & \cdots & -B_{m+1n} & -\frac{V_{mm+1}}{V_{m+1}^2} & \cdots & 0 \\ \vdots & \vdots & \vdots & \vdots & \vdots & \vdots & \vdots & \vdots & \vdots & \vdots & \vdots & \vdots & \vdots & \vdots & \vdots & \vdots & \vdots \\ G_{n1} & G_{n2} & \cdots & G_{nm} & G_{nm+1} & \cdots & G_{nn}^{''} & -B_{n1} & -B_{n2} & \cdots & -B_{nm} & -B_{nm+1} & \cdots & B_{nn}^{''} & 0 & \cdots & -\frac{V_{mn}}{V_n^2} \\ 0 & 0 & \cdots & 0 & 2V_{rm+1} & \cdots & 0 & 0 & 0 & \cdots & 0 & 2V_{mm+1} & \cdots & 0 & 0 & \cdots & 0 \\ 0 & 0 & \cdots & 0 & 0 & \cdots & 0 & 0 & 0 & \cdots & 0 & 0 & \cdots & 0 & \vdots & \vdots & \vdots \\ 0 & 0 & \cdots & 0 & 0 & \cdots & 2V_{rn} & 0 & 0 & \cdots & 0 & 0 & \cdots & 2V_{mn} & 0 & \cdots & 0 \end{bmatrix} \begin{bmatrix} \Delta V_{r1} \\ \Delta V_{r2} \\ \vdots \\ \Delta V_{rm} \\ \Delta V_{rm+1} \\ \vdots \\ \Delta V_{rn} \\ \Delta V_{m1} \\ \Delta V_{m2} \\ \vdots \\ \Delta V_{mm} \\ \Delta V_{mm+1} \\ \vdots \\ \Delta V_{mn} \\ \Delta Q_{m+1} \\ \vdots \\ \Delta Q_n \end{bmatrix}$$

where the amount of PQ buses is denoted by m and PV buses that numbered from $m+1$ to n are placed behind PQ buses in the matrix.

$$B_{kk}^{'} = \begin{cases} B_{kk} - \dfrac{Q_k(V_{rk}^2 - V_{mk}^2) - 2V_{rk}V_{mk}P_k}{(V_{rk}^2 + V_{rk}^2)^2} & k \le m \\ B_{kk} + \dfrac{Q_k}{V_k^2} & k \ge m+1 \end{cases}$$

$$G_{kk}^{'} = \begin{cases} G_{kk} - \dfrac{P_k(V_{rk}^2 - V_{mk}^2) + 2V_{rk}V_{mk}Q_k}{(V_{rk}^2 + V_{rk}^2)^2} & k \le m \\ G_{kk} - \dfrac{P_k}{V_k^2} & k \ge m+1 \end{cases}$$

$$G_{kk}^{''} = \begin{cases} G_{kk} + \dfrac{P_k(V_{rk}^2 - V_{mk}^2) + 2V_{rk}V_{mk}Q_k}{(V_{rk}^2 + V_{rk}^2)^2} & k \le m \\ G_{kk} - \dfrac{P_k}{V_k^2} & k \ge m+1 \end{cases}$$

$$B_{kk}^{''} = \begin{cases} -B_{kk} - \dfrac{Q_k(V_{rk}^2 - V_{mk}^2) - 2V_{rk}V_{mk}P_k}{(V_{rk}^2 + V_{rk}^2)^2} & k \le m \\ -B_{kk} - \dfrac{Q_k}{V_k^2} & k \ge m+1 \end{cases}$$